

Lattice Dynamics of bcc Zirconium

C. Stassis and J. Zarestky

*Ames Laboratory—U. S. Department of Energy, and Department of Physics,
Iowa State University, Ames, Iowa 50011*

and

N. Wakabayashi

Solid State Division, Oak Ridge National Laboratory, Oak Ridge, Tennessee 37830

(Received 17 July 1978)

We have studied the lattice dynamics of bcc Zr at 1400 K. We find that (a) the [111] longitudinal branch plunges rapidly to low frequencies in the vicinity of $q = \frac{2}{3}[111]$ indicating a natural inclination for this metal to undergo a structural transformation to the ω phase, (b) the [110] longitudinal branch is anomalous at the zone boundary, and (c) the condition of elastic isotropy is satisfied to within experimental error. Temperature-dependent elastic peaks were observed in the vicinity of the reciprocal lattice points of the ω phase.

Inelastic neutron scattering experiments have revealed anomalies in the phonon spectra of superconducting transition elements and their compounds that are generally attributed¹ to strong electron-phonon interactions in these metals. As a result considerable effort has been directed towards an understanding of the origin of these anomalies and their relation to the superconducting properties of these metals. The transition elements in the fifth and sixth columns of the periodic table (and in particular Nb) have been extensively studied, since the experiments and their interpretation are made easier by the fact that these elements have the same crystal structure, body-centered cubic. Measurements of the dispersion curves of the high-temperature bcc phases of the transition elements in the fourth column (in particular of bcc Zr), on the other hand, have not been attempted because of the difficulty of growing single crystals of these phases.

The transition elements of the fourth column solidify to a bcc structure (β phase) but all undergo, at temperatures below 1000 K (for Zr 1135 K), a transformation of the martensitic variety to the hcp structure (α phase). There is, however, a competing transformation to the so-called ω phase which occurs both under pressure² in the pure metals as well as upon alloying.³ From the point of view of lattice dynamics, what is interesting about the ω phase is that it can in principle form from the bcc phase through the softening of the $\frac{2}{3}[111]$ longitudinal mode. To characterize the dynamics of the ω transformation and the premonitory structural fluctuations in the bcc phase Moss, Keating, and Axe performed neutron scattering experiments⁴ on $Zr_{0.80}Nb_{0.20}$ and $Zr_{0.92}Nb_{0.08}$ alloys. In these studies⁴ Moss, Keating, and Axe found in particular that elastic peaks in the

vicinity of the ω reflections persisted at temperatures as high as 1300 K and that the dynamical response lacks the average cubic symmetry of the lattice. Clearly, an understanding of the lattice dynamics of the host metal may help in a more fundamental understanding of the ω transformation in these alloys.

Thus measurements of the dispersion curves of the bcc phases of the transition metals of the fourth column are of particular interest since they provide information on how the addition of conduction electrons affects the normal modes of vibration of bcc superconducting elements and on the origin of the ω -phase formation in alloys of the elements of the fourth column. We were successful in growing single crystals of bcc Zr and in this note we report the preliminary results of a study of its dynamical properties by inelastic neutron scattering techniques.

The bcc Zr crystals were grown in a vacuum furnace mounted on the sample goniometer of a triple-axis spectrometer. Single crystals of hcp Zr were cycled through the hcp \rightarrow bcc transformation temperature (~ 1135 K) and then maintained at approximately 1400 K. In a few cases single crystals of bcc Zr of sufficient volume ($1-3$ cm³) for inelastic neutron scattering experiments were found and oriented by standard neutron-diffraction techniques. In all cases the orientation of the bcc crystal relative to that of the parent hcp crystal was found to obey Burgers⁵ crystallographic relations. By using these crystallographic relations and appropriately orienting the hcp parent crystal, we were able to grow bcc crystals in both orientations required to measure the dispersion curves.

A first set of measurements was performed on the sample (crystal I) used in our measure-

ments⁶ on hcp Zr. After completion of the measurements on β -Zr, chemical analysis showed that the crystal had absorbed a rather large amount of oxygen (13 000 ppm). In order to ascertain the effect of O on our results a second set of measurements was performed on a crystal (crystal II) contained in an evacuated thin-wall tantalum crucible. The oxygen content of crystal II after the measurements was found to be 2900 ppm. The measurements on crystal I and crystal II were performed on triple-axis spectrometers at the Ames Laboratory research reactor (ALRR) and the high-flux isotope reactor (HFIR) of the Oak Ridge National Laboratory, respectively.

The dispersion curves determined along the [100], [110], and [111] symmetry directions at 1423 K are shown in Fig. 1. The data obtained with crystal I and crystal II were found to agree to within experimental error. Comparison of Fig. 1 with the dispersion curves of Nb (Ref. 7) and Mo (Ref. 8) which have, respectively, one and two additional electrons outside closed shells reveals **some striking differences** in the phonon spectra of these transition metals. In particular the L[100] and T[100] branches of β -Zr do not cross as in Nb, and unlike the case of Mo no strong anomaly is observed at the point H. The L[110] branch of β -Zr, on the other hand, shows a rather pronounced anomaly in the vicinity of the point N. No such anomaly has been observed in the dispersion curves of the column-V and -VI transition metals or any other bcc metal. Note that the anomaly observed at N in bcc Zr may be related to the anomaly of the zone-center LO[001]

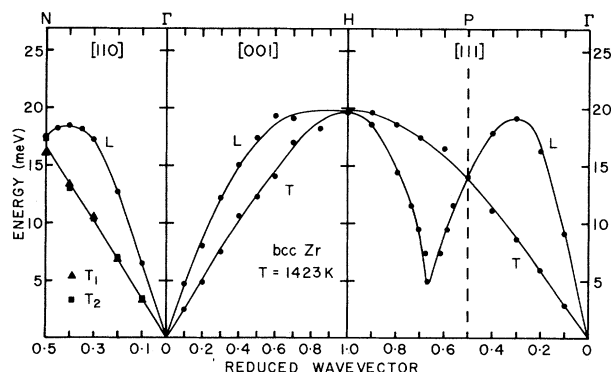


FIG. 1. Dispersion curves along the [100], [110], and [111] symmetry direction of bcc Zr at 1423 K. The frequencies obtained for the two crystals examined in these experiments (see text) were found to agree to within experimental errors. The solid lines were drawn as a guide to the eye.

mode of hcp Zr (Ref. 6) since the (001) hcp plane transforms⁵ to a (110) bcc plane. To within experimental accuracy the $T_1[110]$ and $T_2[110]$ transverse branches are degenerate almost up to the zone boundary. This observation implies in particular that, to within experimental accuracy, the shear moduli c_{44} and $\frac{1}{2}(c_{11} - c_{12})$ are equal, i.e., bcc Zr metal is isotropic with regard to the propagation of elastic waves. From the transition metals of the V and VI columns only tungsten⁹ satisfies the condition of elastic isotropy.

The most unusual feature of the dispersion curves shown in Fig. 1 is the anomalously low frequency of the $\frac{2}{3}[111]$ normal mode. The L[111] branch reaches a maximum of approximately 18 meV at $\xi \approx 0.3$ and then plunges rapidly to below 5 meV in the vicinity of $\xi \approx 0.66$; actually, as a result of instrumental resolution, we were not able to determine the minimum of the dispersion curve. Such a behavior has not been reported for any other bcc element.

It should be pointed out that the precise determination of the frequencies in the vicinity of $\vec{q} = \frac{2}{3}[111]$ is limited not only by instrumental resolution but also by the possible presence of ω -phase material (see below); clearly, if this phase is present the lowest-frequency results may be distorted by Bragg scattering or low- q phonons from this phase. However, we did not observe any anomalous broadening of the neutron groups near $\vec{q} = \frac{2}{3}[111]$. The low-frequency data for the L[111] branch shown in Fig. 1 were obtained by measurements on two crystals (crystals I and II) under different instrumental and resolution conditions. Figure 2 shows phonon groups obtained in four constant-energy-transfer scans through $\vec{q} = \frac{2}{3}[111]$ with crystal II at the HFIR. The frequencies determined from these scans were in excellent agreement with those deduced from similar scans obtained with crystal I at the ALRR.

Comparison of the dispersion curves of β -Zr with those of Nb and Mo reveals that the overall spectrum and the frequency of the $\frac{2}{3}[111]$ mode soften appreciably in going from Mo to β -Zr. More informative in this respect are the results of a detailed investigation by Powell, Martel, and Woods¹⁰ of the lattice dynamics of a series of Nb-Mo alloys. Although the dependence of the measured dispersion curves on alloy composition was found to be rather complicated, an examination of these data (Figs. 1-8 of Ref. 10) shows that the frequency of the $\frac{2}{3}[111]$ mode softens continuously with increasing Nb content in the alloys. Thus the results of the present experiment and

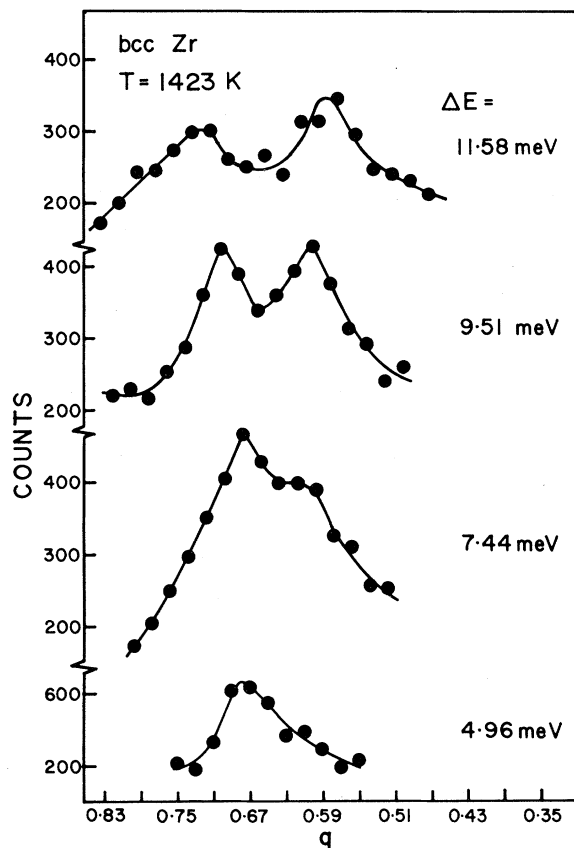


FIG. 2. Constant-neutron-energy-gain (ΔE) scans through $\bar{q} = \frac{2}{3}[111]$ obtained with crystal II at the HFIR. The frequencies obtained from these scans agree to within experimental precision with those deduced from similar scans with crystal I at the ALRR.

those of Powell, Martel, and Woods¹⁰ indicate a continuous softening of the $\frac{2}{3}[111]$ mode as the number of electrons outside closed shells decreases from six for Mo to four for β -Zr. Since as we already mentioned the ω phase can be formed by the softening of this mode, this observation provides support to suggestions¹¹⁻¹⁵ that the transition to the ω phase is electronically driven and proceeds presumably through charge density waves of the appropriate wave vector.

The observed low frequency of the $\frac{2}{3}[111]$ mode motivated a search for superlattice reflections characteristic of the ω phase. Using as reference the bcc lattice of β -Zr these superlattice reflections are at $(h \pm \frac{2}{3}, k \pm \frac{2}{3}, l \pm \frac{2}{3})$ where h , k , and l are the Miller indices of the (h, k, l) parent reflection of the bcc lattice. Elastic peaks in the vicinity of the superlattice positions were found for both crystal samples examined in the present experiments. The widths of these elastic peaks

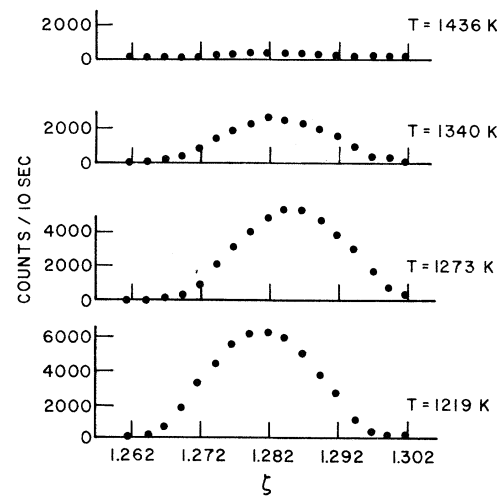


FIG. 3. Temperature dependence of the elastic peak observed in the vicinity of the $(\frac{4}{3}, \frac{4}{3}, \frac{4}{3})$ superlattice reflection of crystal I. The corresponding elastic peak of crystal II was also found to decrease with increasing temperature but not as rapidly as for crystal I (see text).

were only slightly larger than the widths of the parent bcc reflections and the intensities observed could not be accounted for by the measured $\frac{2}{3}\lambda$ contamination of the neutron beam. The elastic peak observed in the vicinity of the $(\frac{4}{3}, \frac{4}{3}, \frac{4}{3})$ superlattice reflection of crystal I is plotted for various temperatures in Fig. 3; the corresponding elastic peak of crystal II was also found to decrease with increasing temperature but not as rapidly as for crystal I. The variation in the intensity of the elastic peaks with changing temperature was found to be reversible. Notice (Fig. 3) that these elastic peaks are displaced toward a lower scattering angle from the exact positions of the superlattice reflections characterizing the ω phase. Thus for both samples examined in the present experiments we observed temperature-dependent elastic peaks in the vicinity of the superlattice positions characterizing the ω phase at temperatures well within the bcc region. Unfortunately no definite conclusion regarding the detailed temperature dependence of these elastic reflections can be drawn before a comprehensive study has been made of the dependence of these elastic peaks not only on the oxygen contamination but also on crystal preparation, heat treatment, and the mosaic structure of the sample at high temperatures. In this connection it should be pointed out that because of secondary extinction effects no information can be obtained from

the intensity of the central peaks without some knowledge of the mosaic spread of the ω -phase material.

Experiments to investigate the detailed structure and temperature dependence of the anomalies observed in bcc Zr, in particular at N and $\frac{2}{3}[111]$ as well as the elastic peaks in the vicinity of the reciprocal lattice points of the ω phase on high-purity samples, are presently in progress at the HFIR of the Oak Ridge National Laboratory. We are also planning to investigate whether the phonons of the $L[111]$ branch exhibit deviations from cubic symmetry as observed by Axe *et al.*⁴ in their study of bcc Zr-Nb alloys.

This work was supported by the U. S. Department of Energy, Office of Basic Energy Sciences, Materials Sciences Division. The authors are grateful to Dr. B. N. Harmon and Dr. W. A. Kamitakahara for many stimulating discussions in the course of this work.

¹H. G. Smith, N. Wakabayashi, and M. Mostoller, in *Superconductivity in d- and f-Band Metals*, edited by D. H. Douglass (Plenum, New York, 1976).

²A. Jayarman, W. Klement, and G. C. Kennedy, *Phys. Rev.* **134**, 664 (1963); B. Olinger and J. C. Jamieson, *High Temp.-High Pressures* **5**, 123 (1973).

³B. A. Hatt and J. A. Roberts, *Acta Metall.* **8**, 575 (1960); B. S. Hickman, *J. Mater. Sci.* **4**, 554 (1969); C. W. Dawson and S. L. Sass, *Metall. Trans.* **1**, 2225 (1970); A. J. Perkins, P. E. Yafee, and R. F. Hehemann, *Metallography* **4**, 303 (1971).

⁴S. C. Moss, D. T. Keating, and J. D. Axe, *Bull. Am. Phys. Soc.* **19**, 321 (1970); S. C. Moss, D. T. Keating, and J. D. Axe, in *Phase Transitions*, edited by L. E. Cross (Pergamon, New York, 1973), p. 179; J. D. Axe, D. T. Keating, and S. C. Moss, *Phys. Rev. Lett.* **35**, 530 (1975).

⁵W. G. Burgers, *Physica (Utrecht)* **1**, 561 (1936); J. W. Glen and S. F. Pugh, *Acta Metall.* **2**, 520 (1954); P. Gaunt and J. W. Christian, *Acta Metall.* **7**, 534 (1959).

⁶C. Stassis, J. Zarestky, D. Arch, O. D. McMasters, and B. N. Harmon, *Phys. Rev. B* **18**, 2632 (1978).

⁷Y. Nakagawa and A. D. B. Woods, *Phys. Rev. Lett.* **11**, 271 (1963).

⁸A. D. B. Woods and S. H. Chen, *Solid State Commun.* **2**, 233 (1964).

⁹S. H. Chen and B. N. Brockhouse, *Solid State Commun.* **2**, 73 (1964).

¹⁰B. M. Powell, P. Martel, and A. D. B. Woods, *Phys. Rev.* **171**, 727 (1968).

¹¹D. de Fontaine, *Acta Metall.* **18**, 275 (1970).

¹²S. C. Moss, D. T. Keating, and J. D. Axe, *Solid State Commun.* **13**, 1465 (1973).

¹³H. E. Cook, *Acta Metall.* **22**, 239 (1974).

¹⁴H. W. Myron, A. J. Freeman, and S. C. Moss, *Solid State Commun.* **17**, 1467 (1975).

¹⁵R. Pynn, *J. Phys. F* **8**, 1 (1978).

Hydrogen-Adsorption-Induced Reconstruction of Tungsten (100): Observation of Surface Vibrational Modes

M. R. Barnes and R. F. Willis

Astronomy Division, European Space Research and Technology Centre, European Space Agency, Noordwijk, The Netherlands

(Received 21 September 1978)

The surface vibrational modes of atomic hydrogen adsorbed on W(100), observed by electron-energy-loss spectroscopy in off-specular directions, indicate bridge bonding at all coverages. The vibrational frequencies show a dependence on the W-H-W bond angle which changes due to reconstruction of the tungsten lattice. The results indicate a W(100) $c[2 \times 2]H$ low-coverage β_2 phase consisting of atoms occupying bridge sites on a $(\sqrt{2} \times \sqrt{2})R 45^\circ$ reconstructed substrate similar to the clean crystal surface at low temperatures.

Low-energy electron-diffraction (LEED) studies of the chemisorption of hydrogen on the (100) face of tungsten show a complex series of changes occurring with increasing coverage. Previous discussions¹ attempted to explain the observations in terms of structural models in which the hydrogen atoms were located at various adsorption sites on an *undistorted* substrate surface. However, whereas the observations are consistent

with H occupying nearest-neighbor bridge-bonding sites W-H-W to form a (1×1) superstructure on the unreconstructed surface at saturation coverage ($\beta_1 \approx 17 \times 10^{14}$ H atoms/cm²), LEED intensity calculations² were found to be incompatible with all structures proposed to date to explain low-coverage adsorption.

The reason would appear to relate to the fact that the clean tungsten surface is unstable at